JOURNAL OF CHEMICAL INFORMATION AND MODELING

Article

pubs.acs.org/jcim

Lid Closure Mechanism of *Yarrowia lipolytica* Lipase in Methanol Investigated by Molecular Dynamics Simulation

Yang Jiang, Lingli Li, Haiyang Zhang, Wei Feng, and Tianwei Tan*

Beijing Key Lab of Bioprocess, College of Life Science and Technology, Beijing University of Chemical Technology, Beijing 100029, China

Supporting Information

ABSTRACT: In nonaqueous organic solvents, lipases can catalyze esterification reactions, which increase their application value. *Yarrowia lipolytica* Lipase (Lip2) possesses potential values in medicine and industrial production. In order to investigate its lid closure mechanism in methanol we performed molecular dynamics (MD) simulations of the open conformation of Lip2 in methanol and hexane, respectively. Simulation results indicated that Lip2 undergoes a greater conformational change in methanol. Principle component analysis showed Lip2 has "double-domain" and "torsion" motion modes in hexane and methanol. By analyzing B-factor and dynamical cross-correlation, region Ser274-Asn288, region Thr106-His126, and region Asp61-Asp67 were found to interact with the lid region (Thr88-Leu105). Furthermore, local restricted MD simulations showed that closure mechanism of Lip2 is "double-lid movement" which is also observed in *Pseudomonas aeruginosa* Lipase (PAL), and we detected two interaction propagation pathways in Lip2 driven by the interaction between Ser274-Asn288 and methanol.

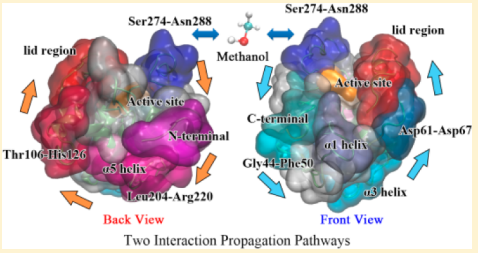

Two Interaction Propagation Pathways

1. INTRODUCTION

Lipases are multifunctional in biocatalysis and have been widely used in biotechnology. The original function of lipases is catalyzing the hydrolysis of triacylglycerols and the synthesis of many non-natural substrates.[1] Lipases have higher thermostability, catalytic activity, and selectivity in organic solvents.[2] They show high catalytic activity at oil−water interface, whereas they show low catalytic activity in aqueous or oil phase.[3] This unique property is known as "interfacial activation".[4] In addition, the polarity of organic solvents also has a significant influence on their catalytic activity.[5] Laane and his co-workers[5] concluded that the enzyme activity was higher in the environment surrounded by nonpolar and midpolar solvents, whereas the lowest activity was expressed in polar solvents. This conclusion has been widely used in solvent selection in enzymatic reactions, but the detailed mechanism was not fully addressed.

Lipases generally adopt an α/β hydrolase fold, which has a core of several parallel β-strands surrounded by α-helices.[6] The active site of lipase is a Ser-His-Asp/Glu catalytic triad and normally covered by a lid.[7] The conformational rearrangements of the lid have been reported to be closely related to the interfacial activation of lipases.[8] With the change of the surrounding environment, the lid undergoes conformational rearrangements to expose (open form) or shield (closed form) the active site.[8,9] Understanding the movement mechanism of lid will be a terrific way to study the catalytic activity of lipases.

Molecular dynamics (MD) simulations have been a useful tool in understanding protein structure and have been used to offer insights into the structure and behavior of the enzymes, especially the lid region.[10−14] James et al.[10] performed MD simulations of *Candida rugosa* lipase (CRL) at hexane/aqueous, octane/aqueous, and decane/aqueous interfaces, respectively. They compared these three systems and concluded that the lid may not just be opening in one set pattern but may vary corresponding to the formations of the interface. Lousa et al.[13] reported an experimental phenomenon called "ligand imprinting" of subtilisin. They studied this phenomenon using MD simulations and pointed out that nonpolar organic solvents can stabilize the open conformation of enzyme. Li et al.[15] studied the conformational changes of *Candida antarctica* lipase B (CALB) in several polar and nonpolar organic solvents. They concluded that polar organic solvent molecules can go into the active pocket and destroy the hydrogen bond network which will result in a loss of lipase activity.

Yarrowia lipolytica Lipase (Lip2) shows high activity in hydrolysis, esterification, and transesterification reactions.[16] Lip2 is now widely used in waste treatment, fine chemistry, traditional food making, citric acid production, and pharmaceutical industry.[17] Recently, the 1.7 Å resolution crystal structure of Lip2 in closed conformation was reported (PDB ID: 3O0D).[18] It is a typical α/β-hydrolase fold and has a conserved Ser-His-Asp catalytic triad (Ser162, His289, and Asp230). Its lid is confirmed to be region Thr88-Leu105. Bordes et al.[18] studied the interfacial activation process of Lip2. They found Lip2 had to undergo two steps of conformational changes to transform itself from closed form to open form. At the octane/water interface, Lip2 adopted a partially open conformation. Only upon subsequent binding of the substrate

Received: January 28, 2014
Published: June 21, 2014

   dx.doi.org/10.1021/ci500163y | *J. Chem. Inf. Model.* 2014, 54, 2033−2041

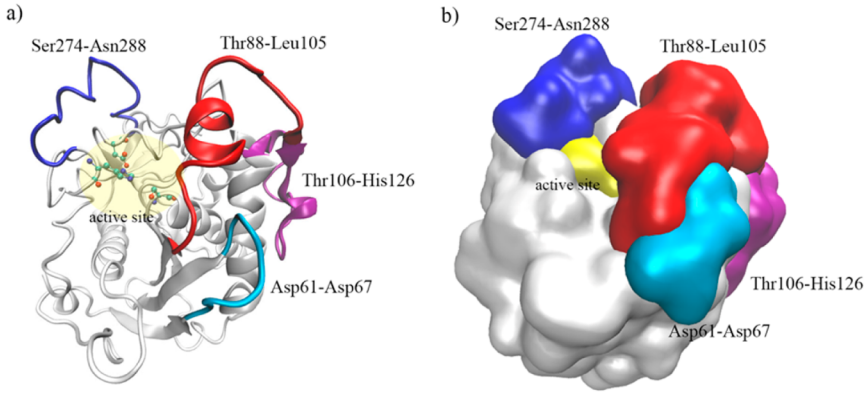

Figure 1. Initial structure of Lip2 in our simulation. a) The initial structure of Lip2 is displayed by the "New Cartoon" model, and its active site residues are represented by a ball and stick model. b) The surface of Lip2 used in our simulation. The active site is colored yellow. Regions Ser274-Asn288, lid (Thr88-Leu105), Thr106-His126, and Asp61-Asp67 are colored blue, red, purple, and cyan, respectively.

did the lipase get a fully open form. Feng et al.[19] studied the activation mechanism of Lip2 immobilized on carbon nanotubes (CNTs). They found the hydrophobic interaction mechanism between Lip2 and CNT and identified the structural path followed by cooperative interactions that originate at the interaction site.

Previous studies which focus on activation mechanism of Lip2 are developing rapidly, but the lid closure mechanism of lipase has not been discussed minutely. Because of the wide usage of lipases in organic solvents, especially in preparation of biodiesel, it is necessary for people to know how the polar organic solvents (e.g., methanol or ethanol) affect the lid of lipase and inactivate it. In this paper, we will discuss the conformational stability, lid motion, and amino acid residues interaction in methanol and hexane and then illuminate the lid closure mechanism of Lip2 in methanol.

2. MATERIALS AND METHODS

2.1. Parameterization of Organic Solvent Molecules. Two organic solvent molecules (methanol and hexane) were used in our simulations. All the geometric parameters and atomic charges were derived by *ab initio* calculation and optimization on the HF/6-31G* level using Gaussian 03.[20] The partial charges were derived by fitting partial charges using the RESP program[21] of AMBER11[22−24] to the electrostatic potential. A periodic box of each solvent was then created. The densities of the boxes were calculated after energy minimization, heating, and equilibration. The results were in good agreement with the experimental densities as shown in Table S1.

2.2. Protein Structure Used. In our study, an open and activated conformation of Lip2 had to be used to start our simulations. Unfortunately, there is no open form crystal structure of Lip2 in the PDB database. According to the previous work of Feng's group,[19,25] Lip2 immobilized on carbon nanotubes had a high activity in experiment. We obtained the final equilibrated structure of Lip2 immobilized on carbon nanotubes from Feng's simulation work[19] to generate the initial structure of open form of Lip2 lipase in our study (Figure 1). Its open degree was 19.91 Å (measurement method see below), which reached the fully open level described by Bordes et al.[18] and was much bigger than that of the closed crystal structure 3O0D (8.5 Å). In Feng's study, substrates could easily access to the active site of this fully open structure, and hydrogen bonds which were vital for the catalysis of lipases were preserved well. Therefore, this structure of Lip2 was considered to be activated and suitable for us to study its lid closure mechanism in methanol. We striped all the organic solvent molecules, Na+ cations, and carbon nanotubes and reserved all the crystal waters around Lip2 in the PDB file.

2.3. Molecular Dynamics Simulations. All molecular dynamics (MD) simulations were performed using the AMBER11 suite. The all-atom ff03 force field[26−28] was used to model lipase and the generalized Amber force field (GAFF)[29] for organic solvent molecules. Lip2 was embedded in a periodic rectangular parallelepiped solvent box containing methanol and hexane, respectively. The solvent molecules left a space of 10 Å around the protein. Several Na+ cations were added to neutralize each system.

An energy minimization was performed to eliminate improper contacts. The steepest descent method was used in the first 5000 steps and the conjugate gradient method in the last 5000 steps. After energy minimization, each system was heated gradually from 0 to 298 K. During the heating steps, position restraints were imposed on the lipase with a force constant of 10.0 kcal/mol/Å^2. Each system was then equilibrated for 200 ps at constant temperature (298 K) and pressure (1 bar) conditions via the Langevin dynamics (the collision frequency is 1.0 ps^{-1}), with a coupling constant of 0.2 ps for both parameters. Production simulations were performed for 100 ns at 298 K and 1 bar using a time step of 2 fs. Electrostatic interactions were calculated using the particle-mesh-Ewald algorithm. The cutoff distance for van der Waals interactions was 10.0 Å. The SHAKE algorithm[30] was applied to all bonds.

Local restricted molecular dynamics simulations were performed to investigate the "double-lid" movement of Lip2. In this method, specified atoms were restricted in Cartesian space using a harmonic potential during the simulation time, and the other atoms were set to be free. The force constant for the positional restraint of each specified atom was set to 100 kcal/mol/Å^2. The details of this simulation will be presented in section 3.3.

2.4. Analytical Methods. The stability of our simulation systems was checked by calculating root-mean-square deviations (RMSds) of backbone atoms (C, CA, N atoms of each residue) and the radius of gyration (RG). RMSds from the open conformation (i.e., initial structure in our simulations) were calculated using least-squares fit. The open degree of active pocket was measured by the distance between Cα atoms

of Ile95 and Ile286. This distance begins from the lid region, passes through active site, and finally ends at an edge of active pocket. Bordes et al.[18] have proved this measurement to be effective for Lip2.

The B-factor was calculated to check the flexibility of each residue. It is derived by the mass-weighted average of atomic (Cα) positional fluctuations (Δr_i^2):[12]

$$Bi = \frac{8\pi^2}{3}\Delta r_i^2 \quad (1)$$

The intraresidue motions in Lip2 were displayed by dynamical cross-correlation map (DCCM),[31] which is a matrix representation of the time-correlated information between protein atoms i and j, (c_{ij}):[32]

$$c_{ij} = \frac{\langle \Delta r_i \cdot \Delta r_j \rangle}{\langle \Delta r_i^2 \rangle^{1/2} \langle \Delta r_j^2 \rangle^{1/2}} \quad (2)$$

The DCCM provided the correlation coefficients for residue displacements along a straight line; positive values were indicative of motions in the same direction (correlated motions), while negative values were indicative of motions in the opposite direction (anticorrelated motions). All the above analyses were calculated using the whole trajectories of production simulations.

The surface areas of simulated protein were calculated using the LCPO algorithm,[33] and the last 10 ns trajectories were used.

Principal component analysis (PCA) was performed to collect the main motion mode of Lip2. It is based on diagonalization of the covariance matrix C_{ij} built from the atomic fluctuations in a MD trajectory from which overall translational and rotational motions have been removed[31,32,34]

$$C_{ij} = \langle (X_i - X_{i,0})(X_j - X_{j,0}) \rangle \quad (3)$$

where X are the x-, y-, and z-coordinates of the Cα atoms fluctuating around their average positions X_0. Then, the eigenvalues and normalized eigenvectors of covariance matrix were computed. Eigenvalues were sorted in descending order. Eigenvectors represented the directions of motions of the atoms, and eigenvalues represented total mean square fluctuation of the system along the corresponding eigenvectors.[34] Relative positional fluctuation (RPF) was then calculated as

$$RPF(n) = \frac{\sum_{i=1}^{n} \lambda(i)}{\sum_{i=1}^{3N} \lambda(i)} \quad (4)$$

where $\lambda(i)$ is the ith eigenvalue, and N is the number of atoms. $RPF(n)$ gives the amount of motion associated in the subspace spanned by the first n eigenvalues. We analyzed one mode generated by the biggest eigenvalue of each system by using "NMWiz" plugin of VMD and ProDy software.[35] To avoid the disturbance of highly flexible residues, PCA was calculated using the coordinates of the first 90 ns trajectories except the first and last 5 residues of the N terminus and the C terminus, respectively.

3. RESULTS AND DISCUSSION

3.1. Overall Conformation. The stability of simulation systems was checked by calculating the RMSds of backbone atoms (Figure S1a) and radius of gyration (RG) (Figure S1b). Obviously, these two systems became stable after 90 ns. The finally equilibrated values (shown in Table S2) of RMSd and RG were defined to be their average values in the last 10 ns. Their finally equilibrated values changed remarkably in different systems. The RMSd and RG became smaller as the polarity of solvent decreased. The decreasing RMSd indicates that Lip2 underwent less conformational change in hexane (nonpolar), and the decreasing value of RG indicates that Lip2 underwent more expansion in methanol (polar).

We calculated the surface area of protein in each system and divided it into two parts, the hydrophilic part and the hydrophobic part. In Table S2, Lip2 in methanol has a big hydrophilic surface area percentage and a small hydrophobic surface area percentage, which are both comparable to that of the crystal structure than the hexane system. Crystal waters were found to be striped by methanol but reserved by hexane. We inferred that methanol molecules destroyed the water layer, and their polar groups had an interaction with Lip2. This may break the hydrophobic packing on the surface of Lip2 and make more hydrophilic residues exposed to solvents (concluded from the bigger hydrophilic surface area percentage). In nonpolar solvents like hexane, the water layer of Lip2 is fully reserved. To some extent, this can keep the hydrophilic and hydrophobic interactions and steady the lipase. These results agree with some previous work[36,37] which elaborated how methanol weakens hydrophobic interactions in proteins.

3.2. Residue Motions. PCA was performed to study the motion mode of Lip2. The eigenvalues and normalized eigenvectors of covariance matrix (eq 3) were calculated. The first 20 eigenvalues and their RPFs are given in Figure S2. The first 20 eigenvalues in each system contribute more than 70% fluctuation of the whole mobility of lipase. The RPF of the biggest eigenvalue reaches 42.0% and 34.8% in hexane and methanol, respectively. Then the most significant motion mode along the eigenvector which was derived from the biggest eigenvalue in each system was drawn as a "porcupine plot"[38,39] shown in Figure 2. At the same time, the MD trajectories were projected on the first principal component and shown in Figure S3. In this mode, Lip2 in hexane shows a "double-domain" motion mode, just like the "breathing" mode described by Cheng et al.[40] These two domains moved toward different directions to keep the active pocket open and make the lipase more compact (Figure 2a and Figure S3a). Lip2 in methanol shows a "torsion" motion mode. The whole lipase rotates clockwise (from its top view) to make it expand and the active pocket trends to close (Figure 2b and Figure S3b). The same results between porcupine plot and projected trajectories indicate that porcupine plot can show us correct results of motion trend, so in the following discussion we will only show the porcupine plot.

The open degree of active pocket is directly shown by the distance plot (Figure S4). In the last 10 ns, the distance between Ile95 and Ile286 reaches a stable value in each system. Obviously, Lip2 has an open (17−18 Å) and closed (10−12 Å) active pocket in hexane and methanol, respectively. In order to study how the active pocket closed, we checked the B-factor of each residue in each system (shown in Figure S5). A big value of the B-factor represents a high flexibility. There is no significant fluctuation of Lip2 in the hexane system. This indicates that in the absence of carbon nanotubes, there is no unusual fluctuation or movement in Lip2, but there are two significant fluctuations in methanol system. One is around region Thr106-His126, and the other is around region Ser274-Asn288. These two regions have a strong relationship with the

dx.doi.org/10.1021/ci500163y | J. Chem. Inf. Model. 2014, 54, 2033−2041

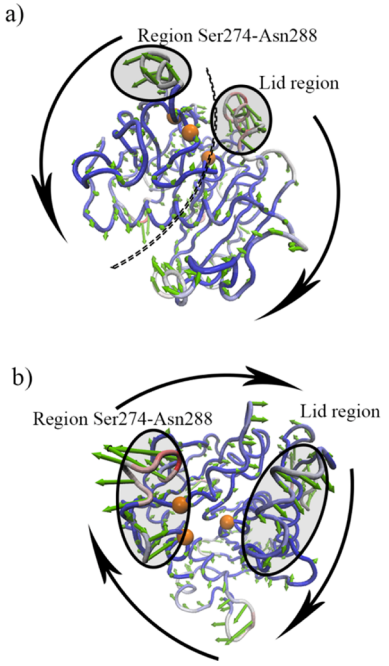

Figure 2. Most significant motion mode of Lip2 in organic solvents. a) The side view of "double-domain" motion mode or "breathing" mode of Lip2 in hexane. The two domains are separated by a dotted line. b) The top view of "torsion" motion mode of Lip2 in methanol. The protein is drawn by a "Tube" model. Its color varies with the increasing mobility of each residue, from cold blue to warm red. The arrows which represent the significant directions of Cα motion are colored green, and their length varies with residue mobility. The residues of active site are represented by orange balls. The two regions (Thr88-Leu105 and Ser274-Asn288) are covered by ellipses. The global motions are represented by black arrows.

lid region (Thr88-Leu105) in 3D space (Figure 1) as well as region Asp61-Asp67 which has been described by Bordes et al.[18] The B-factors of region Thr106-His126 and region Ser274-Asn288 are bigger in methanol than that in hexane. This indicates that the flexibility of these regions may have a relationship with the open degree of active pocket.

Then, we checked the dynamical cross-correlation of these regions in hexane (shown in Figure 3) and methanol (shown in Figure 4). In hexane, region Asp61-Asp67 has a strong correlated motion with the front part of the lid (residue 88-90) and a strong anticorrelated motion with the middle part of the lid (residue 92-94). Region Thr106-His126 has some strong correlated and anticorrelated motions with the lid, but region Ser274-Asn288 only has some weak anticorrelated motions in hexane. In the "double-domain" motion mode, region Asp61-Asp67 moves away from the lid. This makes the front part of the lid move away from Ser162 (correlated motion). Region Thr106-His126 moves outward from the protein and makes the lid move toward Ser162 (anticorrelated motion). Region Ser274-Asn288 moves away from Asp230 and His289. Its directions of motion are mostly perpendicular to the directions of the lid region motion, so we could not find some strong correlated or anticorrelated motions between these two regions; but this mode indeed keeps an active site exposed to solvents.

In methanol system, region Asp61-Asp67, region Thr106-His126, and region Ser274-Asn288 all have stronger dynamical cross-correlations. Opposite to the hexane system, region Asp61-Asp67 moves toward the lid region. Motions of region Asp61-Asp67 (correlated motion) and region Thr106-His126 (anticorrelated motion) make the front part of the lid move toward Ser162 and bury it (Figure 4). The end part of region Ser274-Asn288 moves toward Asp230 and His289 and then buries them. Its front part moves outward, so does the end part of the lid region. These motions make the active pocket close and let us pay attention to region Ser274-Asn288, whose motion feature is similar to the feature of the lid region, so we studied the collaboration of region Ser274-Asn288 and the lid region.

3.3. Double-Lid Movement. If a lipase has two lid regions, it may have a so-called "double-lid" movement. "Double-lid" movement was first investigated by Cherukuvada et al.[41] They performed MD simulations for *Pseudomonas aeruginosa* lipase (PAL) and found it has another lid structure. After analyzing the relationship between the first lid and the second lid using restricted MD simulations, they proposed a theory of "double-lid" movement. Similarly, Wang et al.[42] investigated the catalytic mechanism of T1 lipase and found T1 lipase also had two lids. Barbe et al.[12] investigated the activation mechanism of *Burkholderia cepacia* lipase (BCL). They discussed whether BCL has the "double-lid" movement using restricted MD simulations and studied the influence of side chain atoms. They found the side chain atoms had a great influence on its lid, which was different from Cherukuvada's study. They inferred that the activation mechanism of BCL was not the "double-lid" movement.

According to these studies, we performed local restricted MD simulations of Lip2 in methanol, because Lip2 in methanol undergoes more conformational changes and its lid transforms to close. Our local restricted MD simulation experiment had four groups: The first group had a restriction on all atoms of region Ser274-Asn288 with other atoms free; the second group just on Cα atoms of region Ser274-Asn288; the third group on all atoms of the lid region with other atoms free; the fourth group just on Cα atoms of the lid region. Each of these groups had a methanol solvent box. The constraint force constant was set to 100 kcal/mol/Å^2, and other parameters were the same as in our previous simulation. Because Lip2 in the all-atom free system had almost completely gotten to the closed conformation at 60 ns (the distance between residue Ile95 and residue Ile286 decreased to about 10 Å, Figure S4), the first and second groups were both simulated to 60 ns. The third and fourth groups were both simulated to 40 ns, at which time the distance between residue Ile95 and residue Ile286 of these two groups had already decreased to about 12 Å (Figure S6 b). In order to analyze the relationship between the movements of the lid and region Ser274-Asn288, we compared each of these four groups with the all-atom free system.

3.3.1. Lid Movement Is Triggered by Region Ser274-Asn288. At 60 ns, the distance between residue Ile95 and residue Ile286 of the free system has already decreased to about 10 Å, but the distances of the first two restricted systems both stay between 18 and 19 Å (Figure S6 a). This shows the lid movement is trapped when we restrict the movement of region Ser274-Asn288. No matter if we restrict all atoms of region Ser274-Asn288 or only its Cα atoms, the lid does not move toward region Ser274-Asn288 to change lipase's conformation to the closed form. This shows that it is not only the side chain atoms but also the main chain atoms of region Ser274-Asn288 that influence the movement of the lid.

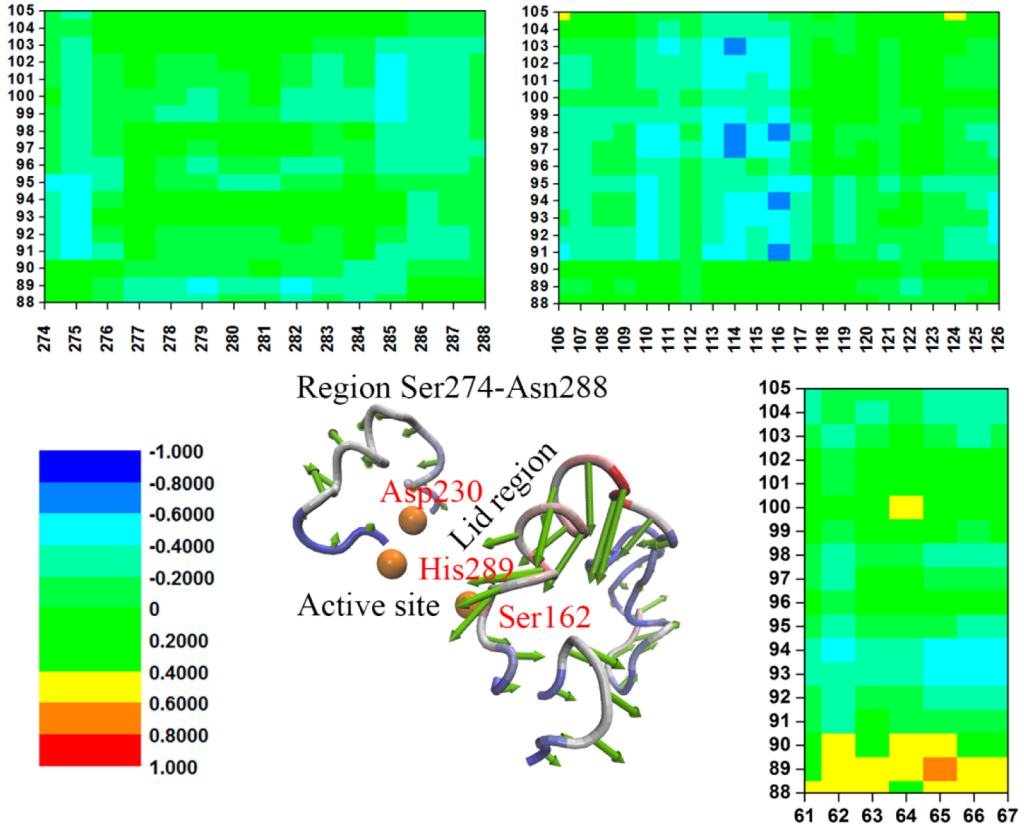

Figure 3. Correlated motion of the lid and its peripheral regions in hexane. Dynamical cross-correlation maps (DCCM) are shown the detail of correlated motion of lid (Thr88-Leu105) and its peripheral regions (Ser274-Asn288, Thr106-His126, and Asp61-Asp67). The numbers of DCCM are indexes of the residues in these two regions. The correlation coefficient between two residues is represented by the color map shown in the left bottom (blue represents the strong anticorrelated motion and red represents the strong correlated motion). These regions are shown in the "Tube" model, and their significant motion mode is shown as green arrows described in Figure 2.

3.3.2. Region Ser274-Asn288 Movement Is Independent of Lid. The distances between residue Ile95 and residue Ile286 of the third and fourth groups both decreased quickly. At about 12 ns, they had already decreased to about 12 Å. The speed of the lid-closing movement in the restricted system was faster than that in the all-atom free system. This is opposite to the result of region Ser274-Asn288 restricted systems (Figure S6). In addition, the side chain of the lid has a small influence on the open degree of active pocket but does not change its closing trend.

In conclusion, the lid movement is triggered by region Ser274-Asn288, but region Ser274-Asn288 movement is independent of the lid. This result is similar to Cherukuvada's study.[41] The side chain atoms of these two regions do not play a key role in their global motion trend, which is different from the conclusion of Barbe's study.[12] We inferred Lip2 (open form) in methanol solvent would have the "double-lid" movement similar to PAL, which may be the closure mechanism of active pocket of Lip2 in methanol solvent.

3.4. Interaction Propagation Pathway. Then we checked the B-factors of each residue in these four restricted systems and the free system (shown in Figure 5). We found some significant changes between the restricted system and the free system. When region Ser274-Asn288 was restricted, no matter on all atoms or just Cα atoms, flexibility of the region Asp61-Asp67 and region Thr106-His126 decreased, and there was a higher flexibility in the end part of the lid region but lower flexibility in its front part. When the lid region was restricted, no matter on all atoms or just Cα atoms, the region Asp61-Asp67, region Ser274-Asn288, and region Thr106-His126 almost kept their flexibility. These indicate that the mobility of region Asp61-Asp67 and region Thr106-His126 are not limited by the lid region. Their motions can impact the conformation change of the lid region via the interactions and movements described in section 3.2.

When region Ser274-Asn288 was restricted, the flexibilities of region Phe206-Arg220 and region Thr106-His126 decreased. In addition, the flexibilities of N-terminal and end part of α5 helix (Trp200-Phe205) increased (seen in Figure 5a, all the names of helices refer to Bordes' work,[18] according to the crystal structure of Lip2:3O0D, similarly hereinafter). These regions kept their flexibilities on free system level in lid restricted systems. Analogous to the above analysis, motion of region Ser274-Asn288 can impact the motions of above regions. According to a previous study,[19] there exists a propagation of hydrophobic interactions among region Phe206-Arg220, the end part of α5 helix (Trp200-Phe205), and the end part of region Thr106-His126. These regions which have strong dynamical cross-correlations (shown in Figure S7a) combine to be an interaction propagation pathway (Pathway I, through region Ser274-Asn288, N-terminal, region Phe206-Arg220, end part of α5 helix, region Thr106-His126 to the lid region). In the case of free lipase, region Ser274-Asn288 can promote the conformation rearrangement of region Phe206-Arg220 and region Thr106-His126, keep the stability

dx.doi.org/10.1021/ci500163y | J. Chem. Inf. Model. 2014, 54, 2033−2041

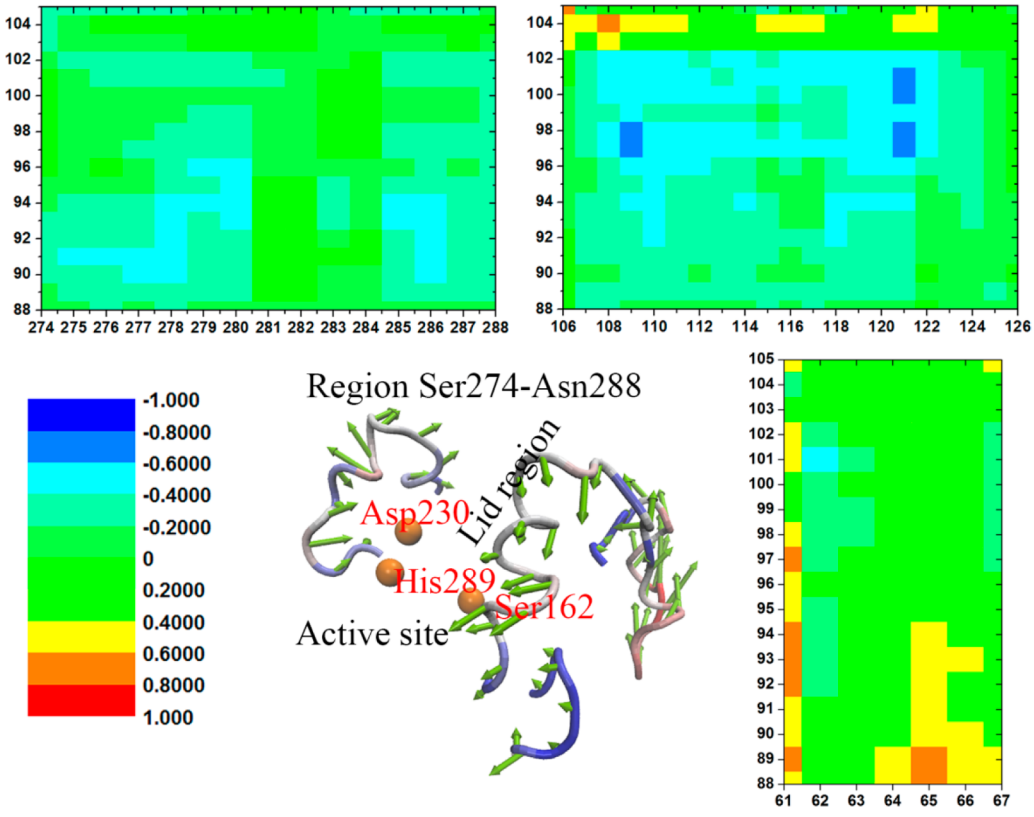

Figure 4. Correlated motion of lid and its peripheral regions in methanol. Dynamical cross-correlation maps (DCCM) and the four specific regions are the same as Figure 3.

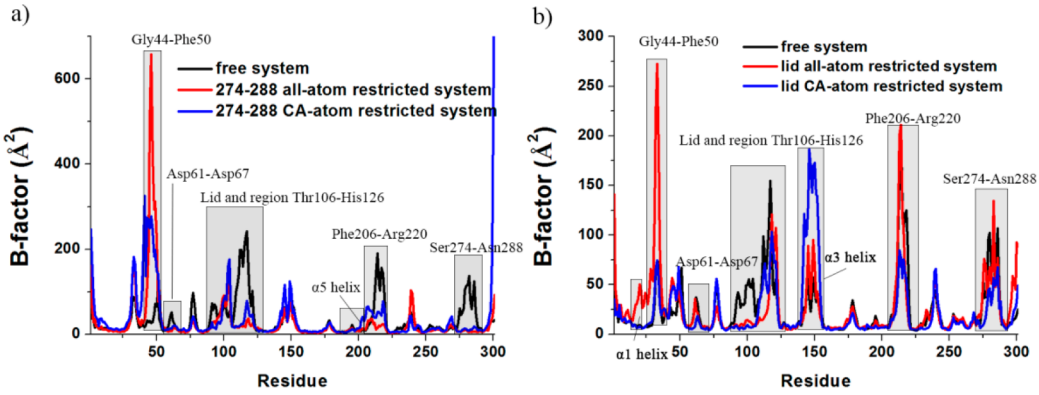

Figure 5. B-factors of each residue in restricted simulation systems. a) The comparison of free system (black), region Ser274-Asn288 all-atom restricted system (red), and region Ser274-Asn288 Cα-atom restricted system (blue). b) The comparison of the free system (black), the lid all-atom restricted system (red), and the lid Cα-atom restricted system (blue). The regions discussed in text are covered by gray rectangles and labeled by their residue names.

of N-terminal and end part of α5 helix (Trp200-Phe205), and propagate the interactions to the lid region.

In addition, C-terminal and region Gly44-Phe50 become more flexible to the response to the increasing polarity of their microenvironment in the Ser274-Asn288 restricted system. The flexibility of α1 helix (Lys20-Ile37) and the end part of α3 helix (Asn138-Gln155) rises when the lid region is restricted (seen in Figure 5b). This may be related with the fast closure of the active pocket in the lid restricted system. These indicate that there must be some related motions among these regions. By carefully analyzing dynamical cross-correlation in the methanol system (shown in Figure S7b), we inferred that there exists another propagation pathway (Pathway II) through region Ser274-Asn288, C-terminal, α1 helix (Lys20-Ile37), region Gly44-Phe50, end part of α3 helix (Asn138-Gln155), region Asp61-Asp67 to the lid region according to their strong dynamical cross-correlations. In the case of free lipase, region Ser274-Asn288 also can promote the conformation rearrangement of α1 helix (Lys20-Ile37), end part of α3 helix (Asn138-Gln155), and region Asp61-Asp67, keep the stability of C-terminal and region Gly44-Phe50, and propagate the interactions to the lid region.

Pathway II and Pathway I form an interaction network around the active pocket to control its closing (shown in Figure 6), through some related movements like the one described in section 3.2. In this interaction network, there are disulfide

dx.doi.org/10.1021/ci500163y | J. Chem. Inf. Model. 2014, 54, 2033−2041

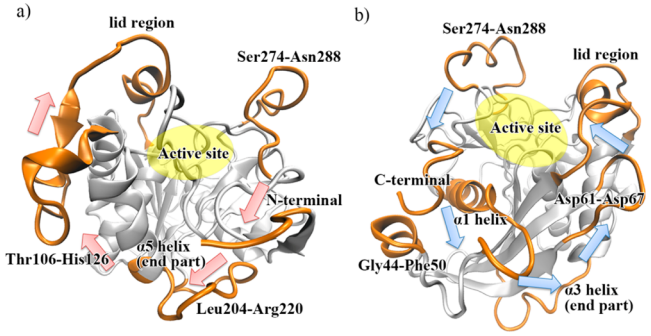

Figure 6. Interaction propagation pathway of Lip2 in methanol. a) Interaction propagation pathway I. b) Interaction propagation pathway II. All of these regions in pathways I and II are orange, and the active pocket is covered by a yellow ellipse. The directions of these two pathways are represented by pink and light blue arrows, respectively.

bonds (e.g., between C-terminal and α1 helix: Cys299-Cys30), hydrogen bonds, salt bridges (e.g., between Phe206-Arg220 and α5 helix: Glu209-Lys203), and van der Waals interactions. In the closure process of Lip2, conformational rearrangement of region Ser274-Asn288 seems to be the root of these interaction propagations. The driving force of this motion and conformational rearrangement may come from its abundant hydrophobic surface (Table 1). Region Ser274-Asn288 propagates its

Table 1. Comparison of the Hydrophilic and Hydrophobic Surface Areas[a] of the Lid Region and Region Ser274-Asn288

	initial structure		final structure[b]	
regions	$SASA_{hydrophilic}$ (Å^2)	$SASA_{hydrophobic}$ (Å^2)	$SASA_{hydrophilic}$ (Å^2)	$SASA_{hydrophobic}$ (Å^2)
lid region	638.6993 (46.25%)	742.1688 (53.75%)	654.2458 (47.75%)	715.9437 (52.25%)
Ser274-Asn288	353.7122 (35.97%)	629.6775 (64.03%)	728.4865 (51.54%)	684.8196 (48.46%)

[a]All the surface areas were calculated using our initial structure via the LCPO algorithm. [b]The final structure was obtained by the average structure of Lip2 during the last 5 ns simulation in the methanol system.

interaction with solvents through pathway I and pathway II to the lid region and makes the active pocket close. The pathways in nonpolar organic solvents like hexane may be interdicted due to the weak interaction between region Ser274-Asn288 and solvents. This is one of the reasons why Lip2 in hexane cannot fully close.

Compared to the previous study[19] which elucidated the activation mechanism of immobilized Lip2, some parts of pathways in our study are the same with the previous pathways. Above all, all of the destinations of these pathways are in the lid region, but the interaction sites and types of these two studies are different. In the activation process, many hydrophobic residues of its carbon nanotube binding site were exposed, but in the inactivation process, many hydrophilic residues of region Ser274-Asn288 were exposed (Table 1). These different interaction types cause different conformational rearrangements of regions in propagation pathways and finally cause different movements, which determine the lid is open or closed. This indicates that Lip2 lipase uses different ways to respond to the changed environments.

4. CONCLUSIONS

In this work we used molecular dynamics simulations to study how the conformation of Lip2 lipase changes in methanol and hexane. The stability of its conformation decreased with the increasing polarity of organic solvents. Methanol molecules could destroy the distribution of crystal waters around the lipase. Their interactions with Lip2 made the whole conformation expand and more hydrophilic residues exposed to solvent. In contrast, hexane may keep the crystal waters around lipase and steady its conformation.

Principle components analysis (PCA) confirmed that Lip2 in methanol may have a "torsion" motion mode which made its structure loose and active pocket close. PCA also confirmed that Lip2 in hexane has a "double-domain" motion mode which made it tight and kept active pocket open. B-factor and dynamical cross-correlation showed that Lip2 in methanol has obvious motions in region Ser274-Asn288 and region Thr106-His126. Using restricted MD simulations, we proved that Lip2 in methanol had the "double-lid" movement which was similar to PAL. Furthermore, we found out two interaction propagation pathways in Lip2 which made its active pocket close in methanol. The major power of the "double-lid" movement might be the motion and conformational rearrangement of region Ser274-Asn288, whose hydrophobic surface area percentage was bigger than lid's so that it had stronger interactions with methanol molecules. This may be the closure mechanism of Lip2 in methanol.

■ ASSOCIATED CONTENT

Supporting Information

Experimental density and simulated density of organic solvents used in simulation. RMSDs of backbone atoms of Lip2 and RG of Lip2 in different organic solvents. The finally equilibrated values of RMSd, RG, and surface area. The first 20 eigenvalues and their relative positional fluctuations (RPFs) in principal component analysis (PCA). The collected Cα trajectories projected along the first principal mode of Lip2 in hexane and methanol systems. The distance between Cα atoms of Ile95 and Ile286 vs simulation time of Lip2 in different solvents. The B-factors of each residue of Lip2 in different solvents. The open degree of active pocket in restricted simulation systems. The dynamical cross-correlation maps (DCCM) of interaction propagation pathways. This material is available free of charge via the Internet at http://pubs.acs.org.

■ AUTHOR INFORMATION

Corresponding Author

*E-mail: twtan@mail.buct.edu.cn.

Notes

The authors declare no competing financial interest.

■ ACKNOWLEDGMENTS

This work was supported by the National Basic Research Program of China (973 program) (2013CB733603, 2011CB710800), the National Nature Science Foundation of China (21390202, 21106005), National High-Tech R&D Program of China (863 Program) (2014AA022101, 2014AA021904). All of our MD simulations were supported by CHEMCLOUDCOMPUTING.

■ ABBREVIATIONS

Lip2, *Yarrowia lipolytica* Lipase 2; MD, molecular dynamics; RMSd, root-mean-square deviation; RG, radius of gyration; DCCM, dynamical cross-correlation map; PCA, principal component analysis; RPFs, relative positional fluctuations

■ REFERENCES

(1) Pandey, A.; Benjamin, S.; Soccol, C. R.; Nigam, P.; Krieger, N.; Soccol, V. T. The realm of microbial lipases in biotechnology. *Biotechnol. Appl. Biochem.* **1999**, *29*, 119−131.

(2) Zaks, A.; Klibanov, A. M. Enzymatic catalysis in organic media at 100 degrees C. *Science* **1984**, *224*, 1249−1251.

(3) Yang, B.; Wu, K.; Liu, B.; Zheng, M.; Cai, J.; Pan, R. Rhizopus arrhizus Lipase Catalyzed Syntheses of Three Esters in Nonaqueous Solvents. *Chin. J. Biochem. Mol. Biol.* **2003**, *5*, 572−575.

(4) Verger, R. 'Interfacial activation'of lipases: facts and artifacts. *Trends Biotechnol.* **1997**, *15*, 32−38.

(5) Laane, C.; Boeren, S.; Vos, K.; Veeger, C. Rules for optimization of biocatalysis in organic solvents. *Biotechnol. Bioeng.* **1987**, *30*, 81−87.

(6) Schrag, J. D.; Cygler, M. Lipases and alpha/beta hydrolase fold. *Methods Enzymol.* **1996**, *284*, 85−107.

(7) Secundo, F.; Carrea, G.; Tarabiono, C.; Gatti-Lafranconi, P.; Brocca, S.; Lotti, M.; Jaeger, K.-E.; Puls, M.; Eggert, T. The lid is a structural and functional determinant of lipase activity and selectivity. *J. Mol. Catal. B: Enzym.* **2006**, *39*, 166−170.

(8) Thomas, A.; Allouche, M.; Basyn, F.; Brasseur, R.; Kerfelec, B. Role of the lid hydrophobicity pattern in pancreatic lipase activity. *J. Biol. Chem.* **2005**, *280*, 40074−40083.

(9) Halimi, H.; De Caro, J.; Carrière, F.; De Caro, A. Closed and open conformations of the lid domain induce different patterns of human pancreatic lipase antigenicity and immunogenicity. *Biochim. Biophys. Acta, Proteins Proteomics* **2005**, *1753*, 247−256.

(10) James, J. J.; Lakshmi, B. S.; Seshasayee, A. S. N.; Gautam, P. Activation of *Candida rugosa* lipase at alkane−aqueous interfaces: A molecular dynamics study. *FEBS Lett.* **2007**, *581*, 4377−4383.

(11) Micaêlo, N. M.; Soares, C. M. Modeling hydration mechanisms of enzymes in nonpolar and polar organic solvents. *FEBS J.* **2007**, *274*, 2424−2436.

(12) Barbe, S.; Lafaquière, V.; Guieysse, D.; Monsan, P.; Remaud-Siméon, M.; André, I. Insights into lid movements of Burkholderia cepacia lipase inferred from molecular dynamics simulations. *Proteins: Struct., Funct., Bioinf.* **2009**, *77*, 509−523.

(13) Lousa, D.; Baptista, A. M.; Soares, C. M. Structural determinants of ligand imprinting: A molecular dynamics simulation study of subtilisin in aqueous and apolar solvents. *Protein Sci.* **2011**, *20*, 379−386.

(14) Lousa, D.; Baptista, A. N. M.; Soares, C. U. M. Analyzing the molecular basis of enzyme stability in ethanol/water mixtures using molecular dynamics simulations. *J. Chem. Inf. Model.* **2012**, *52*, 465−473.

(15) Li, C.; Tan, T.; Zhang, H.; Feng, W. Analysis of the Conformational Stability and Activity of Candida antarctica Lipase B in Organic Solvents Insight from Molecular Dynamics and Quantum Mechanics/Simulations. *J. Biol. Chem.* **2010**, *285*, 28434−28441.

(16) Fickers, P.; Benetti, P. H.; Wache, Y.; Marty, A.; Mauersberger, S.; Smit, M.; Nicaud, J. M. Hydrophobic substrate utilisation by the yeast Yarrowia lipolytica, and its potential applications. *FEMS Yeast Res.* **2005**, *5*, 527−543.

(17) Fickers, P.; Marty, A.; Nicaud, J. M. The lipases from *Yarrowia lipolytica*: Genetics, production, regulation, biochemical characterization and biotechnological applications. *Biotechnol. Adv.* **2011**, *29*, 632−644.

(18) Bordes, F.; Barbe, S.; Escalier, P.; Mourey, L.; André, I.; Marty, A.; Tranier, S. Exploring the Conformational States and Rearrangements of *Yarrowia lipolytica* Lipase. *Biophys. J.* **2010**, *99*, 2225−2234.

(19) Feng, W.; Sun, X.; Ji, P. Activation mechanism of Yarrowia lipolytica lipase immobilized on carbon nanotubes. *Soft Matter* **2012**, *8*, 7143−7150.

(20) Frisch, M. J.; Trucks, G. W.; Schlegel, H. B.; Scuseria, G. E.; Robb, M. A.; Cheeseman, J. R.; Montgomery, J. A., Jr.; Vreven, T.; Kudin, K. N.; Burant, J. C.; Millam, J. M.; Iyengar, S. S.; Tomasi, J.; Barone, V.; Mennucci, B.; Cossi, M.; Scalmani, G.; Rega, N.; Petersson, G. A.; Nakatsuji, H.; Hada, M.; Ehara, M.; Toyota, K.; Fukuda, R.; Hasegawa, J.; Ishida, M.; Nakajima, T.; Honda, Y.; Kitao, O.; Nakai, H.; Klene, M.; Li, X.; Knox, J. E.; Hratchian, H. P.; Cross, J. B.; Bakken, V.; Adamo, C.; Jaramillo, J.; Gomperts, R.; Stratmann, R. E.; Yazyev, O.; Austin, A. J.; Cammi, R.; Pomelli, C.; Ochterski, J. W.; Ayala, P. Y.; Morokuma, K.; Voth, G. A.; Salvador, P.; Dannenberg, J. J.; Zakrzewski, V. G.; Dapprich, S.; Daniels, A. D.; Strain, M. C.; Farkas, O.; Malick, D. K.; Rabuck, A. D.; Raghavachari, K.; Foresman, J. B.; Ortiz, J. V.; Cui, Q.; Baboul, A. G.; Clifford, S.; Cioslowski, J.; Stefanov, B. B.; Liu, G.; Liashenko, A.; Piskorz, P.; Komaromi, I.; Martin, R. L.; Fox, D. J.; Keith, T.; Al-Laham, M. A.; Peng, C. Y.; Nanayakkara, A.; Challacombe, M.; Gill, P. M. W.; Johnson, B.; Chen, W.; Wong, M. W.; Gonzalez, C.; Pople, J. A. In Gaussian, Inc.: Wallingford, CT, 2004.

(21) Bayly, C. I.; Cieplak, P.; Cornell, W.; Kollman, P. A. A well-behaved electrostatic potential based method using charge restraints for deriving atomic charges: the RESP model. *J. Phys. Chem.* **1993**, *97*, 10269−10280.

(22) Case, D.; Darden, T.; Cheatham III, T.; Simmerling, C.; Wang, J.; Duke, R.; Luo, R.; Walker, R.; Zhang, W.; Merz, K. AMBER 11; University of California: San Francisco, 2010, 142.

(23) Case, D. A.; Cheatham, T. E., III; Darden, T.; Gohlke, H.; Luo, R.; Merz, K. M., Jr.; Onufriev, A.; Simmerling, C.; Wang, B.; Woods, R. J. The Amber biomolecular simulation programs. *J. Comput. Chem.* **2005**, *26*, 1668−1688.

(24) Pearlman, D. A.; Case, D. A.; Caldwell, J. W.; Ross, W. S.; Cheatham, T. E.; DeBolt, S.; Ferguson, D.; Seibel, G.; Kollman, P. AMBER, a package of computer programs for applying molecular mechanics, normal mode analysis, molecular dynamics and free energy calculations to simulate the structural and energetic properties of molecules. *Comput. Phys. Commun.* **1995**, *91*, 1−41.

(25) Tan, H.; Feng, W.; Ji, P. Lipase immobilized on magnetic multi-walled carbon nanotubes. *Bioresour. Technol.* **2012**, *115*, 172−176.

(26) Duan, Y.; Wu, C.; Chowdhury, S.; Lee, M. C.; Xiong, G.; Zhang, W.; Yang, R.; Cieplak, P.; Luo, R.; Lee, T. A point-charge force field for molecular mechanics simulations of proteins based on condensed-phase quantum mechanical calculations. *J. Comput. Chem.* **2003**, *24*, 1999−2012.

(27) Jorgensen, W. L.; Maxwell, D. S.; Tirado-Rives, J. Development and testing of the OPLS all-atom force field on conformational energetics and properties of organic liquids. *J. Am. Chem. Soc.* **1996**, *118*, 11225−11236.

(28) Lee, M. C.; Duan, Y. Distinguish protein decoys by using a scoring function based on a new AMBER force field, short molecular dynamics simulations, and the generalized born solvent model. *Proteins: Struct., Funct., Bioinf.* **2004**, *55*, 620−634.

(29) Wang, B.; Merz, K. M., Jr. A fast QM/MM (quantum mechanical/molecular mechanical) approach to calculate nuclear magnetic resonance chemical shifts for macromolecules. *J. Chem. Theory Comput.* **2006**, *2*, 209−215.

(30) Ryckaert, J.-P.; Ciccotti, G.; Berendsen, H. J. Numerical integration of the cartesian equations of motion of a system with constraints: molecular dynamics of *n*-alkanes. *J. Comput. Phys.* **1977**, *23*, 327−341.

(31) Arcangeli, C.; Bizzarri, A. R.; Cannistraro, S. Molecular dynamics simulation and essential dynamics study of mutated plastocyanin: structural, dynamical and functional effects of a disulfide bridge insertion at the protein surface. *Biophys. Chem.* **2001**, *92*, 183−199.

(32) Ichiye, T.; Karplus, M. Collective motions in proteins: a covariance analysis of atomic fluctuations in molecular dynamics and normal mode simulations. *Proteins: Struct., Funct., Bioinf.* **1991**, *11*, 205−217.

(33) Weiser, J.; Shenkin, P. S.; Still, W. C. Approximate atomic surfaces from linear combinations of pairwise overlaps (LCPO). *J. Comput. Chem.* **1999**, *20*, 217−230.
(34) Sanjeev, B.; Vishveshwara, S. Essential dynamics and sidechain hydrogen bond cluster studies on eosinophil cationic protein. *Eur. Phys. J. D: At., Mol. Opt. Phys.* **2002**, *20*, 601−608.
(35) Bakan, A.; Meireles, L. M.; Bahar, I. ProDy: protein dynamics inferred from theory and experiments. *Bioinformatics* **2011**, *27*, 1575−1577.
(36) Hwang, S.; Shao, Q.; Williams, H.; Hilty, C.; Gao, Y. Q. Methanol strengthens hydrogen bonds and weakens hydrophobic interactions in proteins−a combined molecular dynamics and NMR study. *J. Phys. Chem. B* **2011**, *115*, 6653−6660.
(37) Zhu, L.; Yang, W.; Meng, Y. Y.; Xiao, X.; Guo, Y.; Pu, X.; Li, M. Effects of organic solvent and crystal water on γ-chymotrypsin in acetonitrile media: observations from molecular dynamics simulation and DFT calculation. *J. Phys. Chem. B* **2012**, *116*, 3292−3304.
(38) Tai, K.; Shen, T.; Börjesson, U.; Philippopoulos, M.; McCammon, J. A. Analysis of a 10-ns molecular dynamics simulation of mouse acetylcholinesterase. *Biophys. J.* **2001**, *81*, 715−724.
(39) Haider, S.; Parkinson, G. N.; Neidle, S. Molecular dynamics and principal components analysis of human telomeric quadruplex multimers. *Biophys. J.* **2008**, *95*, 296−311.
(40) Cheng, Y.; Zhang, Y.; McCammon, J. A. How does activation loop phosphorylation modulate catalytic activity in the cAMP-dependent protein kinase: A theoretical study. *Protein Sci.* **2006**, *15*, 672−683.
(41) Cherukuvada, S. L.; Seshasayee, A. S. N.; Raghunathan, K.; Anishetty, S.; Pennathur, G. Evidence of a double-lid movement in Pseudomonas aeruginosa lipase: insights from molecular dynamics simulations. *PLoS Comput. Biol.* **2005**, *1*, e28.
(42) Wang, Y.; Wei, D.-Q.; Wang, J.-F. Molecular dynamics studies on T1 lipase: insight into a double-flap mechanism. *J. Chem. Inf. Model.* **2010**, *50*, 875−878.